

**Science**AAAS**Ischemia Opens Neuronal Gap Junction  
Hemichannels**Roger J. Thompson, *et al.*  
*Science* **312**, 924 (2006);  
DOI: 10.1126/science.1126241

***The following resources related to this article are available online at  
www.sciencemag.org (this information is current as of November 20, 2008 ):***

**Updated information and services**, including high-resolution figures, can be found in the online version of this article at:

<http://www.sciencemag.org/cgi/content/full/312/5775/924>

**Supporting Online Material** can be found at:

<http://www.sciencemag.org/cgi/content/full/312/5775/924/DC1>

A list of selected additional articles on the Science Web sites **related to this article** can be found at:

<http://www.sciencemag.org/cgi/content/full/312/5775/924#related-content>

This article **cites 23 articles**, 12 of which can be accessed for free:

<http://www.sciencemag.org/cgi/content/full/312/5775/924#otherarticles>

This article has been **cited by** 45 article(s) on the ISI Web of Science.

This article has been **cited by** 15 articles hosted by HighWire Press; see:

<http://www.sciencemag.org/cgi/content/full/312/5775/924#otherarticles>

This article appears in the following **subject collections**:

Neuroscience

<http://www.sciencemag.org/cgi/collection/neuroscience>

Information about obtaining **reprints** of this article or about obtaining **permission to reproduce this article** in whole or in part can be found at:

<http://www.sciencemag.org/about/permissions.dtl>

## References and Notes

- J. Whangbo, C. Kenyon, *Mol. Cell* **4**, 851 (1999).
- J. Harris, L. Honigberg, N. Robinson, C. Kenyon, *Development* **122**, 3117 (1996).
- J. Whangbo, J. Harris, C. Kenyon, *Development* **127**, 4587 (2000).
- S. J. Salsler, C. Kenyon, *Nature* **355**, 255 (1992).
- A. G. Fraser *et al.*, *Nature* **408**, 325 (2000).
- M. N. Seaman, J. M. McCaffery, S. D. Emr, *J. Cell Biol.* **142**, 665 (1998).
- M. Verges *et al.*, *Nat. Cell Biol.* **6**, 763 (2004).
- B. F. Horazdovsky *et al.*, *Mol. Biol. Cell* **8**, 1529 (1997).
- H. C. Korswagen, *Bioessays* **24**, 801 (2002).
- C. J. Thorpe, A. Schlesinger, J. C. Carter, B. Bowerman, *Cell* **90**, 695 (1997).
- M. A. Herman, H. R. Horvitz, *Development* **120**, 1035 (1994).
- K. M. Cadigan, M. P. Fish, E. J. Rulifson, R. Nusse, *Cell* **93**, 767 (1998).
- F. J. Staal, B. M. Burgering, M. van de Wetering, H. C. Clevers, *Int. Immunol.* **11**, 317 (1999).
- J. Noordermeer, F. Meijlink, P. Verrijzer, F. Rijsewijk, O. Destree, *Nucleic Acids Res.* **17**, 11 (1989).
- A. P. McMahon, R. T. Moon, *Cell* **58**, 1075 (1989).
- J. Roose *et al.*, *Nature* **395**, 608 (1998).
- S. Hoppler, J. D. Brown, R. T. Moon, *Genes Dev.* **10**, 2805 (1996).
- J. Vallin *et al.*, *J. Biol. Chem.* **276**, 30350 (2001).
- T. Kadowaki, E. Wilder, J. Klingensmith, K. Zachary, N. Perrimon, *Genes Dev.* **10**, 3116 (1996).
- K. Tanaka, Y. Kitagawa, T. Kadowaki, *J. Biol. Chem.* **277**, 12816 (2002).
- C. E. Rocheleau *et al.*, *Cell* **90**, 707 (1997).
- D. Panakova, H. Sprong, E. Marois, C. Thiele, S. Eaton, *Nature* **435**, 58 (2005).
- J. E. Sulston, H. R. Horvitz, *Dev. Biol.* **56**, 110 (1977).
- We thank C. McNulty, H. Clevers, and R. Plasterk for critically reading the manuscript; J. Ahringer, A. Fire, C. Haft, D. Hermand, R. Moon, J. Smith, and C. Wolkow for reagents; B. Bowerman, J. Kuipers, W. Stoorvogel, and M. van de Wetering for help and advice; Shohei Mitani (National Bioresource Project for the Nematode, Tokyo) for deletion mutants; and the *Caenorhabditis* Genetic Center (University of Minnesota, Minneapolis) for strains. This work was supported by the Dutch Cancer Foundation, the EU FP6 program Cells into Organs (H.C.K.), and EU grant QLRT-2000-01275 (O.D.).

## Supporting Online Material

www.sciencemag.org/cgi/content/full/1124856/DC1

Materials and Methods

Figs. S1 to S4

Tables S1 to S6

References

11 January 2006; accepted 13 April 2006

Published online 27 April 2006;

10.1126/science.1124856

Include this information when citing this paper.

# Ischemia Opens Neuronal Gap Junction Hemichannels

Roger J. Thompson, Ning Zhou, Brian A. MacVicar\*

Neuronal excitotoxicity during stroke is caused by activation of unidentified large-conductance channels, leading to swelling and calcium dysregulation. We show that ischemic-like conditions [ $O_2$ /glucose deprivation (OGD)] open hemichannels, or half gap junctions, in neurons. Hemichannel opening was indicated by a large linear current and flux across the membrane of small fluorescent molecules. Single-channel openings of hemichannels (530 picosiemens) were observed in OGD. Both the current and dye flux were blocked by inhibitors of hemichannels. Therefore, hemichannel opening contributes to the profound ionic dysregulation during stroke and may be a ubiquitous component of ischemic neuronal death.

The rapid decrease of  $O_2$  and glucose in the infarct region of ischemic tissue can trigger necrotic cellular death within a few minutes as a result of  $Ca^{2+}$ ,  $Na^+$ ,  $K^+$ , and  $Cl^-$  dysregulation (1, 2). An unexplored contributor to unregulated ionic fluxes in neurons is hemichannel opening. Hemichannels are open unapposed half gap junctions that form large-conductance channels and allow flux of ions and molecules (<1 kD). Connexin (Cx) hemichannels function physiologically during inhibition in the outer retina (3), and metabolic inhibition or divalent cation free solutions open Cx43 hemichannels in astrocytes and cardiomyocytes (4–6). Pyramidal neurons in the central nervous system do not express connexins but express pannexin 1 (Px1), which forms gap junctions and hemichannels in oocytes, and can open as a hemichannel at negative resting membrane potentials or in physiological  $Ca^{2+}$  concentrations (7–9).

Our recording conditions were designed to isolate nonselective channels by including a cocktail of blockers against glutamate receptors and voltage-dependent  $K^+$ ,  $Na^+$ , and  $Ca^{2+}$

channels (10). OGD activated a large inward current in acutely isolated hippocampal neurons within  $9.7 \pm 1.2$  min (Fig. 1, A and E; range, 3 to 19 min;  $n = 19$ ). The current had a large amplitude ( $-74.7 \pm 16$  pA/pF at  $-60$  mV) versus the control ( $-4.4 \pm 1.1$  pA/pF), a linear current-voltage ( $I-V$ ) relationship, and a reversal potential near 0 mV (Fig. 1, B and E). The current declined (Fig. 1B) if  $O_2$ /glucose was returned within  $\sim 5$  min of activation (about 15 min after OGD). However, longer durations of OGD (>20 min) resulted in irreversible current activation, neuronal swelling, and membrane breakdown.

The amplitude and linear  $I-V$  of the OGD-activated current suggested activation of hemichannels. To determine hemichannel involvement, we tested the gap junction/hemichannel blocker carbenoxolone (Cbx). After OGD activated the current, Cbx (100  $\mu$ M) was applied and block was observed (Fig. 1C, top trace, and Fig. 1D). In other experiments, the current was not induced when Cbx was applied concomitantly with OGD. Lanthanum chloride ( $La^{3+}$ ; 100  $\mu$ M), which blocks Cx hemichannels, significantly ( $P = 0.042$ ) reduced the amplitude of the OGD-activated current (Fig. 1C, lower trace, and Fig. 1E).

We eliminated the possibilities that the acid-sensitive ion channel ASIC1a (11) and the large-pore purinergic P2X7 receptor contribute to the OGD-activated current. ASIC1a and P2X7 ac-

tivation were unlikely because extracellular pH was maintained at 7.4 and the isolated neurons were constantly perfused at  $\sim 4$  ml/min to prevent the accumulation of secreted molecules (10). Nevertheless, amiloride (100  $\mu$ M, to block ASIC1a channels) or brilliant blue G (BBG; 10  $\mu$ M, to block P2X7 receptors) were bath-applied after current activation or concomitantly with OGD; both failed to affect the large OGD-activated current (Fig. 1F).

After inhibition of the OGD-activated hemichannel by Cbx or  $La^{3+}$ , a small residual current remained (Fig. 1, D and E) that was consistent with the transient receptor potential (TRP) family—specifically, TRPC4 or TRPC5 homomeric channels—because this current had a doubly rectifying  $I-V$  relationship and was augmented by 100  $\mu$ M  $La^{3+}$ . TRP channels have been reported to be activated by OGD and cyanide in cultured cortical neurons (12). We chose to focus the remainder of our investigation on the hemichannel because the very large amplitude of this current would make it a major contributor to ionic dysregulation during OGD.

If the large current in OGD is from hemichannel opening, then influx or efflux of gap junction/hemichannel permeable dyes should be measurable in neurons. Acutely isolated hippocampal neurons were loaded with calcein green AM (Fig. 2A), a largely nonreactive green fluorescent dye with a molecular weight of 0.66 kD that is known to cross gap junctions (13). In control solutions, calcein did not leak from acutely isolated neurons because fluorescence was stable (control; Fig. 2B). In OGD, calcein fluorescence decreased steadily (Fig. 2, A, B, and D), indicating that ischemia triggered dye efflux. The OGD-induced dye efflux was not affected by antagonists to glutamate receptors and ion channels (10) [Fig. 2D, OGD + blockers +  $D,L$ -2-amino-5-phosphonovaleric acid (APV)]. If dye efflux was mediated by hemichannel opening, Cbx should block it. Figure 2C shows examples from three different hippocampal neurons where dye efflux was blocked by Cbx; data from a number of neu-

Department of Psychiatry and Brain Research Centre, University of British Columbia, Vancouver, British Columbia V6T 2B5, Canada.

\*To whom correspondence should be addressed. E-mail: bmacvica@interchange.ubc.ca

rons are summarized in Fig. 2D. In neuron 1 in Fig. 2C, the neuron was concomitantly exposed to Cbx and OGD, and dye loss was not observed (Fig. 2A, lower panels). In neuron 2, Cbx and OGD were applied simultaneously and Cbx was removed after 35 min; only then did

the calcein fluorescence decrease. Finally, in neuron 3, dye efflux was inhibited by a transient exposure to Cbx. The strong Cbx sensitivity indicates that the decrease in dye signal was not due to photobleaching or to a loss of plasma membrane integrity.

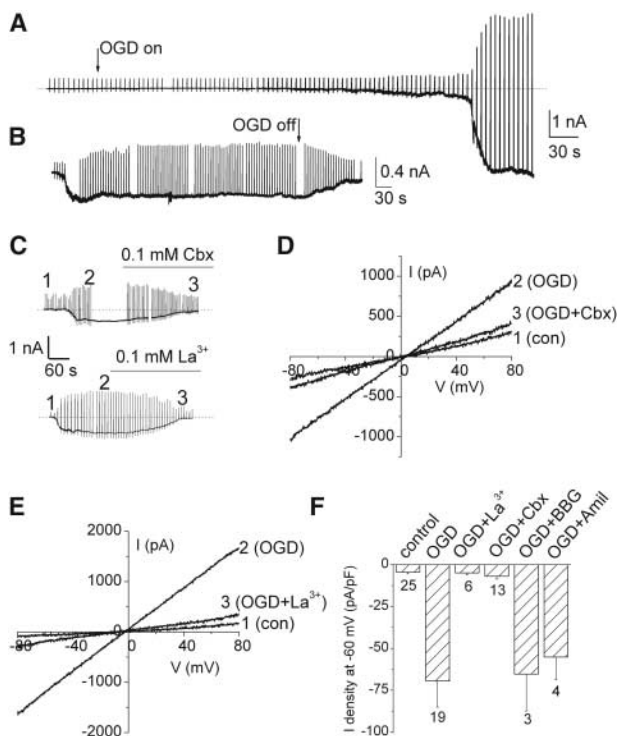


**Fig. 1. Effects of OGD on hippocampal neurons.** (A) Voltage-clamp recording of an acutely isolated rat hippocampal neuron showing activation of a large inward current during ischemia (OGD). The spike-like events are 150-ms voltage ramps from -80 to 80 mV. (B) Return to control solutions within 5 min of activation of the large current resulted in reversal. (C) The hemichannel blockers Cbx and La<sup>3+</sup> blocked the OGD-activated inward current. The numbers above each trace indicate the voltage ramps shown in (D) and (E). (D) The OGD-activated current was blocked by Cbx. (E) La<sup>3+</sup> also blocked the OGD-activated current. (F) Average inward current density at -60 mV (the number of cells is indicated under each bar).

We next used two-photon laser scanning microscopy of identified yellow fluorescent protein-positive (YFP<sup>+</sup>) cortical neurons (10, 14) to measure the influx of another gap junction permeable dye, sulforhodamine 101 (SR101). SR101 is normally completely excluded from neurons but is a selective and stable marker of astrocytes in situ (15). YFP<sup>+</sup> neurons imaged at least 100 μm from the surface of a 400-μm brain slice did not stain with SR101 under control conditions (Fig. 3A). The YFP (green neurons) and red (SR101 in the bath) signals did not overlap. However, after exposure of brain slices to OGD for 12 min, SR101 loading of YFP<sup>+</sup> neurons was observed (Fig. 3, A to C), as indicated by the merging of the YFP and SR101 signals (yellow). YFP-negative neurons also loaded with SR101 during OGD (Fig. 3A).

If SR101 loading in situ was due to hemichannel opening by OGD, as predicted by the in vitro calcein efflux data, then the hemichannel blocker Cbx should abolish SR101 loading. As a semiquantitative measure of dye influx, the intensity of SR101 inside the YFP<sup>+</sup> neuron was subtracted from that for the same sized region outside of the neuron and normalized. Thus, a negative number indicates a higher extracellular SR101 fluorescence relative to that inside the neuron. The average time course (Fig. 3B) shows clearly that SR101 loading of neurons occurred only during OGD, and that this was blocked by Cbx. Neither

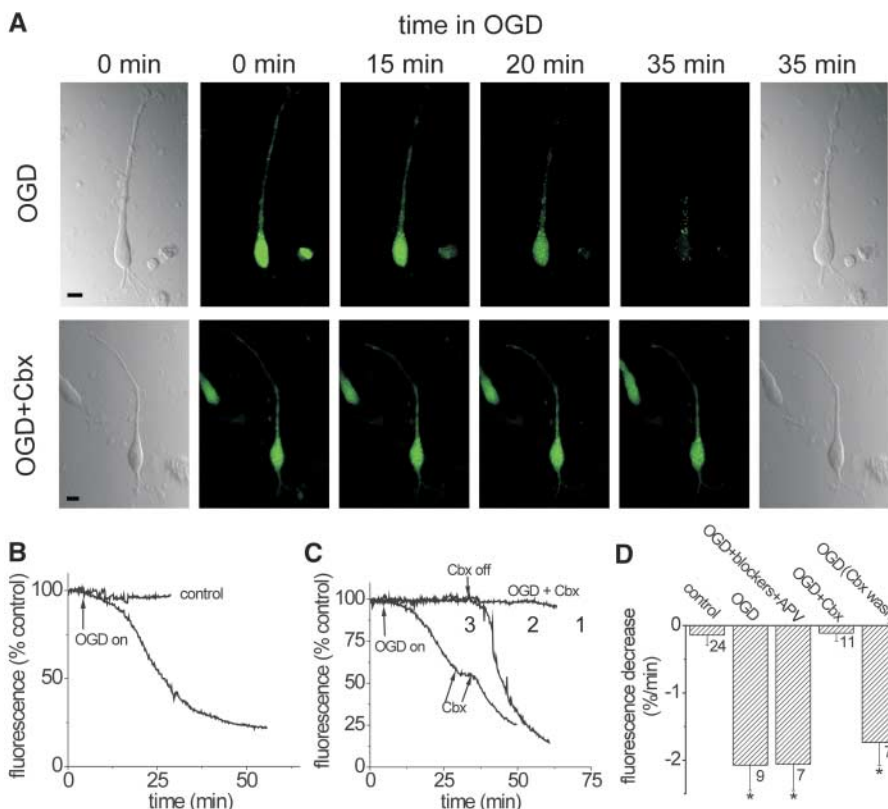


**Fig. 2. Ischemia-mediated efflux of small molecules from neurons.** (A) Confocal images of a calcein-loaded, acutely isolated hippocampal neuron. OGD resulted in rapid calcein efflux, which was inhibited by the hemichannel blocker Cbx (bottom row). Scale bars, 10 μm. (B) Calcein fluorescence during control and OGD. Each trace represents data from different neurons, expressed as the percentage of the average control fluorescence. (C) Calcein fluorescence from three separate neurons exposed to OGD (OGD on) in the presence of Cbx for variable times as indicated. Cbx prevented dye loss from the neurons. (D) Average calcein fluorescence decrease, calculated as the slope over 5-min periods.

BBG nor kynurenic acid plus APV included with the cocktail of blockers (10) (OGD + blockers + APV) prevented the SR101 staining of identified neurons, indicating that P2X7 and ionotropic glutamate receptors were not involved (Fig. 3C).

The most likely candidate for the proteins constituting OGD-activated hemichannels in pyramidal neurons is Pxl, because it may be the only gap junction protein expressed in these cells (9, 16). Cx36, Cx45, and Cx52 are unlikely to contribute to the hemichannel current because they are closed by negative membrane potentials and physiological  $\text{Ca}^{2+}$  concentrations (8, 11). The conductance of homomeric Pxl (550 pS) (7) is at least 200 pS larger than

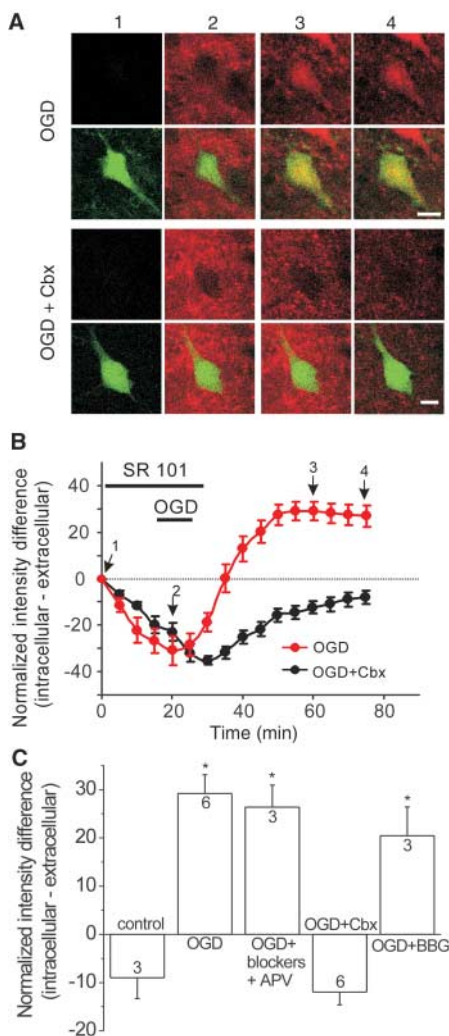


**Fig. 3.** Effect of OGD on dye loading in situ. **(A)** Two-photon laser scanning microscopy images of YFP<sup>+</sup> mouse cortical neurons in a 400- $\mu\text{m}$  brain slice. SR101 (red; first and third rows) was excluded from the cells under control conditions. Dye influx occurred during OGD (top rows) and was prevented by hemichannel block (Cbx, bottom rows). Scale bar, 10  $\mu\text{m}$ . **(B)** Time course of SR101 intensity inside YFP<sup>+</sup> neurons. **(C)** Average SR101 difference intensities (outside minus inside) 45 min after OGD.

those reported for connexin hemichannels (17). We therefore performed cell-attached single-channel recording from acutely isolated hippocampal neurons to determine the single-channel conductance of OGD-activated channels.

Openings of large-conductance channels (Fig. 4A) were rare under control conditions, as illustrated by the single peak in the all-points amplitude histogram of Fig. 4D and the low open probability (Fig. 4G, control). In OGD, 5 of 13 patches showed activation of two or more large-conductance channels (Fig. 4, B and C). The average single-channel current amplitude and conductance were  $-31.6 \pm 2.2$  pA ( $n = 5$ ) and  $527 \pm 36$  pS at  $-60$  mV (Fig. 4D). Open probability was increased by a factor of 4.5 over control (Fig. 4G). The channels had a linear  $I$ - $V$  plot with a reversal potential near 0 mV (Fig. 4E). Full single-channel transitions were observed (Fig. 4F), which is a biophysical criterion indicating the presence of bona fide large-conductance channels and not

the summated openings of many smaller ones (18). All of these single-channel biophysical properties are similar to those of homomeric Pxl hemichannels expressed in oocytes (7). Finally, Cbx was bath-applied after appearance of the large channels and resulted in a slowly reversible block in all four cell-attached patches that were tested (Fig. 4, C, D, and G).

We propose that ischemic insults open Pxl hemichannels, and that this is a central component of the increased plasma membrane permeability leading to neuronal necrosis. Pxl hemichannel opening may have several severe physiological consequences for neurons. First, these nonselective cation channels could mediate the dysregulated ionic fluxes that are known to occur during ischemia (1, 2). Other pathways may be involved, such as ASIC1a channels (11), voltage-dependent  $\text{Na}^+$  channels (19),  $N$ -methyl-D-aspartate (NMDA) receptors (20), and TRP channels (12). However, we argue that the extremely large amplitude of the

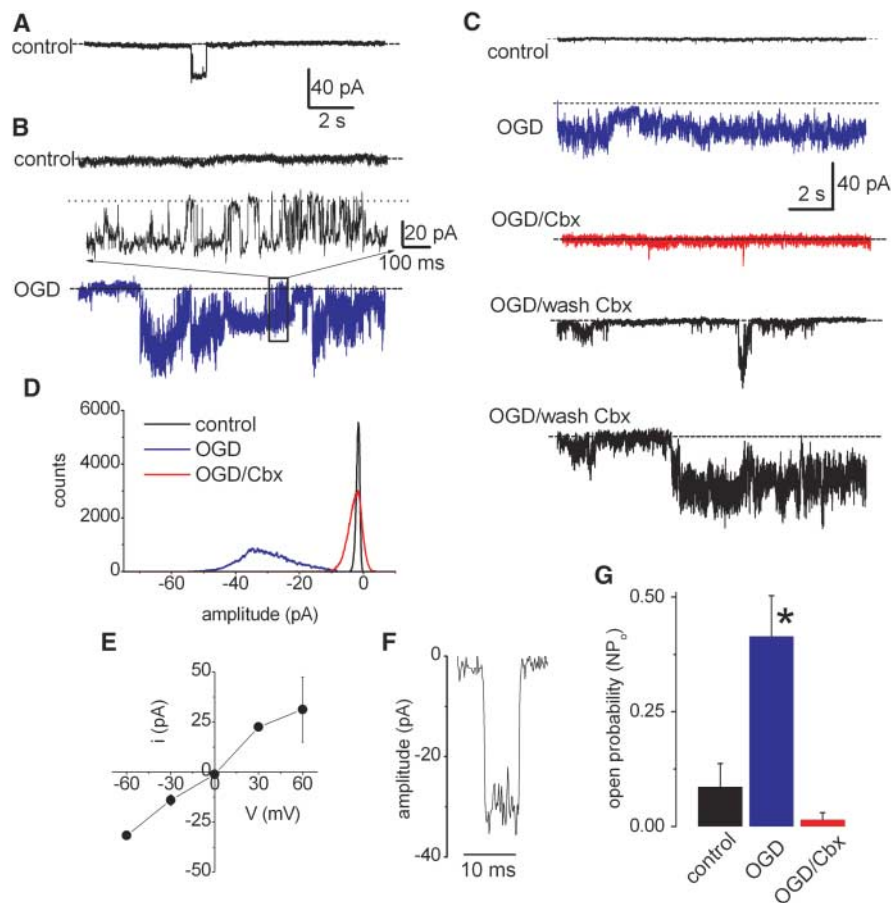


**Fig. 4.** OGD activates single large-conductance channels. **(A)** Cell-attached patch recording (duration 15 s) under control conditions. **(B)** Recordings from a hippocampal neuron under control (black) and during exposure to OGD (blue). The boxed region is expanded to show large single-channel transitions. **(C)** Cell-attached recordings from a neuron showing hemichannel activation by OGD (blue), inhibition by carbenoxolone (Cbx; red), and reversal after washout of Cbx. **(D)** All-points amplitude histograms from the traces in (C), showing the closed (control) and open amplitudes (OGD). **(E)** Average  $I$ - $V$  plot of OGD-activated hemichannels from five different neurons. **(F)** A single opening (and closing) of the hemichannel in OGD. **(G)** Hemichannel open probability ( $\text{NP}_o$ ) was significantly increased during OGD ( $n = 5$ ) and blocked by Cbx.

hemichannel makes it a major contributor to ionic dysregulation in ischemia. Second, Pxl hemichannel opening may result in efflux of glucose and adenosine triphosphate (ATP), further compromising the neuron's recovery from an ischemic insult. Consistent with this was our observation that fluorescent dyes became membrane-permeable only during OGD. Hemichannels are putative conduits for ATP release from astrocytes (21) and in the cochlea (22). Third, the large amplitude of the Pxl hemichannel current at holding potentials near the neuron's resting membrane potential ( $\sim -60$  mV) indicates that these currents likely contribute substantially to "anoxic depolarization," a poorly understood but well-recognized and key component of ischemic neuronal death (2, 23, 24). Therefore, hemichannel opening may be an important new pharmacological target to prevent neuronal death in stroke.

#### References and Notes

1. A. J. Hansen, *Physiol. Rev.* **65**, 101 (1985).
2. P. Lipton, *Physiol. Rev.* **79**, 1431 (1999).
3. M. Kamermans *et al.*, *Science* **292**, 1178 (2001).
4. J. E. Contreras *et al.*, *Proc. Natl. Acad. Sci. U.S.A.* **99**, 495 (2002).
5. R. P. Kondo, S. Y. Wang, S. A. John, J. N. Weiss, J. I. Goldhaber, *J. Mol. Cell. Cardiol.* **32**, 1859 (2000).
6. H. Li *et al.*, *J. Cell Biol.* **134**, 1019 (1996).
7. L. Bao, S. Locovei, G. Dahl, *FEBS Lett.* **572**, 65 (2004).
8. R. Bruzzone, M. T. Barbe, N. J. Jakob, H. Monyer, *J. Neurochem.* **92**, 1033 (2005).
9. R. Bruzzone, S. G. Hormuzdi, M. T. Barbe, A. Herb, H. Monyer, *Proc. Natl. Acad. Sci. U.S.A.* **100**, 13644 (2003).
10. See supporting material on Science Online.
11. J. Gao *et al.*, *Neuron* **48**, 635 (2005).
12. M. Aarts *et al.*, *Cell* **115**, 863 (2003).
13. C. Tomasetto, M. J. Neveu, J. Daley, P. K. Horan, R. Sager, *J. Cell Biol.* **122**, 157 (1993).
14. G. Feng *et al.*, *Neuron* **28**, 41 (2000).
15. A. Nimmerjahn, F. Kirchhoff, J. N. Kerr, F. Helmchen, *Nat. Methods* **1**, 31 (2004).
16. G. Sohl, S. Maxeiner, K. Willecke, *Nat. Rev. Neurosci.* **6**, 191 (2005).
17. J. C. Saez, M. A. Retamal, D. Basilio, F. F. Bukauskas, M. V. Bennett, *Biochim. Biophys. Acta* **1711**, 215 (2005).
18. R. J. Thompson, M. H. Nordeen, K. E. Howell, J. H. Caldwell, *Biophys. J.* **83**, 278 (2002).
19. M. L. Fung, G. G. Haddad, *Brain Res.* **762**, 97 (1997).
20. H. Benveniste, J. Drejer, A. Schousboe, N. H. Diemer, *J. Neurochem.* **43**, 1369 (1984).
21. C. E. Stout, J. L. Costantin, C. C. Naus, A. C. Charles, *J. Biol. Chem.* **277**, 10482 (2002).
22. H. B. Zhao, N. Yu, C. R. Fleming, *Proc. Natl. Acad. Sci. U.S.A.* **102**, 18724 (2005).
23. T. R. Anderson, C. R. Jarvis, A. J. Biedermann, C. Molnar, R. D. Andrew, *J. Neurophysiol.* **93**, 963 (2005).
24. G. G. Somjen, *Physiol. Rev.* **81**, 1065 (2001).
25. Supported by the Canadian Institutes for Health Research and the Canadian Stroke Network. B.A.M. has a Tier 1 Canada Research Chair in Neuroscience and a Michael Smith Foundation for Health Research distinguished scholar award. We thank Y.-T. Wang, C. C. Naus, and T. Snutch for critical reading of the manuscript.

#### Supporting Online Material

www.sciencemag.org/cgi/content/full/312/5775/924/DC1  
Materials and Methods

14 February 2006; accepted 31 March 2006  
10.1126/science.1126241

## Hypothalamic mTOR Signaling Regulates Food Intake

Daniela Cota,<sup>1</sup> Karine Proulx,<sup>1</sup> Kathi A. Blake Smith,<sup>1</sup> Sara C. Kozma,<sup>2</sup> George Thomas,<sup>2</sup> Stephen C. Woods,<sup>1</sup> Randy J. Seeley<sup>1\*</sup>

The mammalian Target of Rapamycin (mTOR) protein is a serine-threonine kinase that regulates cell-cycle progression and growth by sensing changes in energy status. We demonstrated that mTOR signaling plays a role in the brain mechanisms that respond to nutrient availability, regulating energy balance. In the rat, mTOR signaling is controlled by energy status in specific regions of the hypothalamus and colocalizes with neuropeptide Y and proopiomelanocortin neurons in the arcuate nucleus. Central administration of leucine increases hypothalamic mTOR signaling and decreases food intake and body weight. The hormone leptin increases hypothalamic mTOR activity, and the inhibition of mTOR signaling blunts leptin's anorectic effect. Thus, mTOR is a cellular fuel sensor whose hypothalamic activity is directly tied to the regulation of energy intake.

A subset of neurons in the central nervous system (CNS) plays a role in regulating both blood plasma fuel levels and nutrient intake (1, 2). An emerging concept is that specific neuronal populations integrate fuel availability signals with signals mediated by hormones such as leptin (3). However, the signaling pathways that are involved are poorly understood.

In peripheral cells, the mammalian mTOR signaling pathway integrates nutrient signals with hormonal signals to control growth and development (4, 5). mTOR is a highly conserved serine-threonine kinase, which, in the presence of mitogens and available nutrients (including amino acids), stimulates protein synthesis and inhibits autophagy (6). In vitro, cellular levels of adenosine triphosphate (ATP)

increase mTOR signaling, and mTOR itself is thought to serve as an ATP sensor (7). mTOR thus functions as a checkpoint by which cells sense and decode changes in energy status, which in turn determines the rate of cell growth and proliferation (6). Complete loss of TOR function is lethal in mice (8); in *Drosophila*, defects in TOR signaling result in the formation of smaller cells in all tissues (9). Conversely, increased or otherwise aberrant mTOR activity has been linked to the development of cancer, diabetes, and obesity (10, 11). As is consistent with the development of these diseases, the activation of the mTOR pathway is markedly elevated in the liver and in the skeletal muscle of insulin-resistant obese rats maintained on a high-fat diet (12), whereas the absence of the downstream mTOR target [S6 kinase 1 (S6K1)] protects against diet-induced obesity and enhances insulin sensitivity in mice (13). Given these observations, we hypothesized that mTOR might integrate cellular fuel status

with hormonal-related signaling in specific populations of neurons that use this information to regulate food intake.

To test this hypothesis, we used antibodies to localize mTOR and two downstream targets of mTOR action [S6K1 and S6 ribosomal protein (S6) (5, 6)] in the rat brain. Consistent with previous work (14), antibodies recognizing total mTOR had a ubiquitous distribution in the CNS, and there was scattered expression of specific phosphorylation of mTOR at Ser<sup>2448</sup> (pmTOR) in extra-hypothalamic areas, including the hippocampus, thalamus, and cortex. In the hypothalamus, pmTOR was highly localized in the paraventricular (PVN) and arcuate (ARC) nuclei (fig. S1A) (15). Likewise, total S6K1 stained broadly throughout the CNS, whereas the hypothalamic expression of the activated form of S6K1, phosphorylated at Thr<sup>389</sup> (pS6K1), was also largely limited to the PVN and ARC. Further, dual labeling for pmTOR and pS6K1 revealed that they are localized in the same cells in both of these regions (fig. S1B). Although most of these cells appear to be neurons, some may be glia.

The ARC contains at least two populations of neurons that are linked to the regulation of energy balance and whose activity is regulated by leptin: (i) orexigenic neurons that express both neuropeptide Y (NPY) and agouti-related peptide (AgRP) and (ii) anorexigenic neurons that express proopiomelanocortin (POMC) and cocaine- and amphetamine-regulated transcript (CART). Both pmTOR and pS6K1 were found in  $\sim 90\%$  of ARC NPY/AgRP neurons (Fig. 1A), whereas only 45% of ARC POMC/CART neurons revealed phosphorylation of these proteins (Fig. 1B).

We next investigated whether changes in the body's energy status modulate mTOR signaling

<sup>1</sup>Department of Psychiatry, <sup>2</sup>Department of Genome Science, University of Cincinnati, Genome Research Institute, 2170 East Galbraith Road, Cincinnati, OH 45237, USA.

\*To whom correspondence should be addressed. E-mail: Randy.Seeley@uc.edu